Structural, magnetic and electrical properties of nickelthin films deposited on Si (100) substrates by pulsed laser deposition

M. N. Rizwan[a,*], C. Bell[b], M. A. Kalyar[a], A. R. Makhdoom[c], M. Anwar-ul-Haq[a], E. Gilory[b]
[a]*Department of Physics, University of Sargodha, Sargodha 40100, Pakistan*
[b]*School of Physics, University of Bristol, Tyndall Avenue, BS8 1TL, UK*
[c]*Department of Natural Sciences and Humanities, Rachna College of Engineering and Technology, UET, Lahore*

Nickel thin films have been deposited on silicon (100) substrates by pulsed laser deposition at various substrate temperatures, T_s, in the range 100 - 700 ºC. X-ray diffraction analysis confirms nickel phases are present for T_s in the range 100 - 300 ºC, while above 500 ºC Ni-Si phases were observed. The grain size and roughness of thin films were in the range 30 nm - 590 nm and 4.3 - 15.7 nm respectively for thickness of the films is in the range 45 nm - 100 nm. Systematic variation with T_s was found for these morphological parameters, as well as the ratio of the remnant to saturation magnetic moment, magnetic coercivity and magnetoresistance.

(Received October 23, 2020; Accepted May 1, 2021)

Keywords: Nickel thin films, Pulsed laser deposition, Vander Pauw method, Electrical resistivity and magnetoresistance

1. Introduction

Nickel thin films can be used for a variety of applications including magnetic recording media, magneto caloric refrigeration, and as catalyst for carbon nanotube growth [1-4]. During the last few decades, several groups focused on the growth of nickel thin films on the silicon [6-8] because of their use in the fabrication of ohmic contacts and interconnect of CMOS devices. There have been various studies of microstructure, mechanical and electrical properties using sputtering [6-10], thermal evaporation [11,12] chemical bath deposition [13] as well as pulsed laser deposition (PLD). Hattar *et al,* (2008) deposited nickel thin films on the rock salt by pulsed laser deposition and investigated that large grains cause defects like twins, dislocation lines, small dislocation drops and stacking–fault tetrahedral which strongly influenced the structure and macroscopic mechanical properties [14]. Anca Largeanu *et al* (2011) deposited nickel thin films on steel substrates by using pulsed laser deposition at room temperature to 400 ºC. The smooth growth of film was reported at high temperature [5].

In the present studies, we employed PLD to deposit the nickel thin films on silicon (100) substrates. Pulsed laser deposition is widely used technique to grow thin films from few nanometers to micrometers with easy, simple and rapid process in clean environment. The films were grown in base vacuum at 1×10^{-7} mbar at four different substrate temperatures. Various properties of the Ni thin films such as micro structural, magnetic and electrical properties strongly depend on the substrate temperature. These properties can be enhanced due to improvement in the crystallinity at higher substrate temperature. The effect of substrate temperature on the morphology, thickness and grain size has been investigated. The electrical (sheet resistance, electrical resistivity) and magnetic properties (coercivity, saturated magnetization and magnetic residual ratio) have been studied as a function of substrate temperature.

[*] Corresponding author: rizwannawazsial@gmail.com

2. Experimental

PLD of Ni films was performed in a stainless-steel chamber with a base vacuum of 1.1×10^{-7} mbar. The output from the third harmonics (355nm) of Nd: YAG Laser (Q-smart 850, Quantal) with repetition rate 10 Hz, pulse duration 5 ns, laser fluence 2.4×10^{10} watt/cm^2 was focused on rotating Ni-target (99.99% pure, Testborne UK) by a quartz convex lens (f = 50 cm). The resulting plume of the ablated Ni-material was deposited on Si (100) surface having dimension (10×10×0.5) mm^3 placed at 4 cm normal to the target. Substrates were carefully cleaned by acetone and ethanol. Both the substrate and target were set in continuous rotation throughout the deposition process of 45 minutes. Four substrate temperatures, T_s were utilized: 100 ºC, 300 ºC, 500 ºC and 700 ºC keeping all other deposition parameters constant.

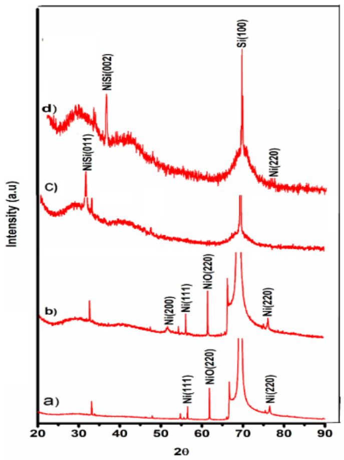

Fig. 1. XRD data of nickel thin films deposited on Si -substrates at T_s of (a) 100 ºC℃, (b) 300 ºC (c) 500 ºC and (d) 700 ºC. Various reflections are labeled.

Room temperature x-ray diffraction (XRD) and x-ray reflectivity (XRR) were employed for the structural analysis and for the measurement of thickness of nickel thin films respectively, using CuKα (wavelength = 1.5418Å) as a x-ray source. Atomic force microscopy (AFM) was used to study the surface morphology and topography of the thin films, and estimate the grain size and roughness. Magnetic measurements were made with Vibrating sample magnetometer (VSM) at room temperature and ultrasonic wire bonding with Al-Si wires in Vander Pauw geometry was used to determine the electrical properties, including the anisotropic magnetoresistance.

3. Results and discussion

Structural and morphological analysis of thin films was carried by XRD, SEM and AFM. Fig. 1 shows the XRD spectra of the films deposited for various *Ts*. For T_s = 100 ºC, the diffraction peaks at 56.5º and 76.5º correspond to (111) and (220) reflections of nickel respectively [10, 15]. Whereas the peak observed at 61.84º is identified as the (220) reflection of NiO [16]. For *Ts* = 300 ºC the (200) reflection of Ni is additionally observed at 52.0º [10, 15, 17]. These data confirm the polycrystalline structure of thin film at deposition temperature in the range 100 - 300 ºC. At higher T_s = 500 ºC- 700 ºC, no reflections corresponding to Ni or NiO were observed, but instead clear evidence of the formation of a Ni-Si phase: the peak at 31.9º corresponds to (011) of NiSi verified by the card No (38-0844) (for *Ts* = 500 ºC) and similarly the NiSi (002) reflection corresponds to peak at 36.4º (at *Ts* = 700 ºC) verified by reflection JCPDS card No (03-1069). The presence of nickel silicon phases at higher deposition temperature is assumed to be due to diffusion and intermixing of Ni with the Si substrate and formation of NiSi phase is similar to that as reported by Tasi *et.al* [18].

3.1. Atomic force microscopy

Atomic force microscopy (AFM) was used to study the surface topography by scanning the thin films in tapping mode. Fig. 2 shows the AFM results including the roughness, grain size and representative scan of film texture. Fig. 2(a) monotonically increased with T_s from ~30 nm to ~ 600 nm over the range of T_s studied, concomitantly the root mean square (RMS) roughness (estimated via a scanned area of (5×5) μm) increased from ~ 4 nm to 16 nm. The grain size and surface morphology of the film are shown in Figure 2(b-c). The correlation between grain size and roughness is reasonably given the enhanced adatom mobility at higher T_s; similar results are reported previously [7]. The thickness of thin films grown at different substrate-temperature was estimated by using X-ray reflectometry (XRR), and the variation with *Ts* is shown in Figure 2(b). Thickness of thin film increased at higher T_S which is responsible for the formation of large grain growth due to the higher thermal energy. The particle /species of ablated material diffuse to form the big grain or density of the material on the surface of substrate increases and as a result thickness of thin film increases [19].

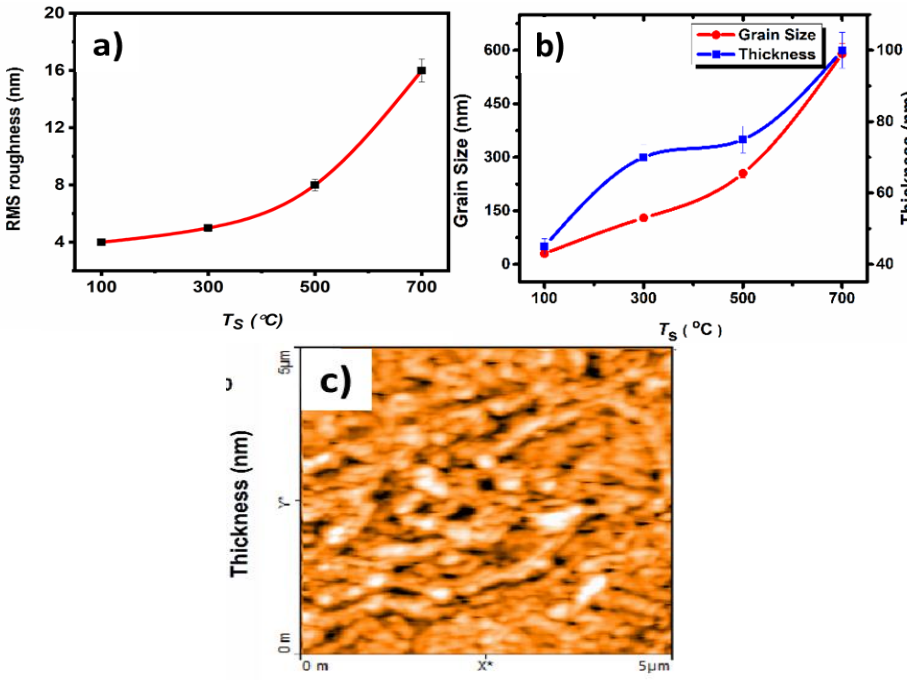

Fig. 2. (a) RMS –roughness, and (b) Grain size, thickness and of thin films as a function of T_S, lines are a guide to the eye. (c) Representative AFM image of a nickel thin film for T_s = 500 °C.

3.2. Magnetic and transport measurements

Magnetic measurements were made at room temperature using a vibrating sample magnetometer with the applied field, *H*, in the plane of all samples. The M-H data for various T_s are shown in Fig. 3(a). We note that the data for T_s = 700 °C is significantly more noisy. The variation of magnetic coercive field (H_c) versus T_s is shown in Figure 3(b). While the latter show a clear monotonic decrease with T_s, the form of H_c (T_s) is less clear, with the value of H_c at T_s = 300 °C data being anomalous as reported earlier [20]. The enhanced roughness and thickness of the films at higher T_s reduces the shape anisotropy which tends to make the in-plane direction a relatively easy axis. Therefore, at higher roughness and thickness the films show more hard axis behavior. The nucleation sites support the growth of crystal structure and grain size increases and this effect causes a reduction in the H_C and M_S of thin films.

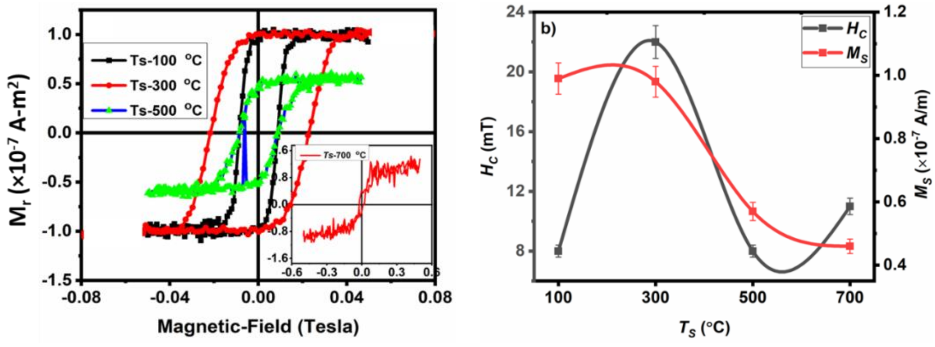

Fig. 3. (a) Room temperature M-H plots of nickel thin films for various T_s. Inset: data for Ts = 700 ºC. (b) M_S and H_c Vs T_s.

AFM image also confirms the increase in the grain size with increased substrate temperature. The x-ray diffraction (XRD) micrographs of deposited nickel thin films show that at low substrate temperature (100 ºC -300 ºC) films are rich in nickel. Therefore, nickel thin films grown at low substrate temperature have a high value of the magnetic moment, residual magnetic ratio and saturated magnetization. But at high deposition temperature 500 ºC-700 ºC, poorer crystallinity of Ni is observed and NiSi phases were formed which causes a decrease in magnetization. At higher deposition temperature, the nickel diffuses into silicon substrate as a result NiSi is formed (as confirmed by XRD). The saturated magnetization and magnetic moment were estimated (0.995 - 0.468) $\times 10^{-7}$ (A/m) and (0.984 - 0.372) $\times 10^{-7}$ (A-m^2) respectively at T_S varied from 100 ºC -700 ºC.

The sheet resistance was measured using Vander Pauw geometry and the longitudinal resistivity, ρ_{xx}, was calculated using the thickness obtained from the XRR data. The resistivity of the films initially increases from 0.82μ Ω-m$\times 10^{-6}(\Omega\text{-m})$to 0.86 μ Ω-m $\times 10^{-6}(\Omega\text{-m})$with increasing T_s from 100- 300 ºC and is significantly lower than 2 - 2.6 μ Ω-m reported by Poyang Motamedi *et.al* at similar deposition temperature [21].$\times 10^{-6}(\Omega\text{-m})$ But further increase in T_s of 500 ºC resistivity sharply reduced to 0.10 μΩ-m due to improvement of crystallinity and is close to that of bulk Ni 0.07μΩ-m [22]. Presumably this trend is a competition between the increase in grain size at higher T_s, which lowers ρ_{xx}, and the increase in roughness and Si inter-diffusion which would increase ρ_{xx}. The variation of electrical resistivity with T_S is illustrated in Fig. 4(b). The magnetoresistance (AMR) was also measured in the longitudinal configuration at room temperature when current passed in a direction longitudinal and transverse relative to the magnetic field. The AMR in both geometries decreased as *Ts* increased, and lies in the ranges (1.06 - 0.009) % as shown in Fig. 4(a).

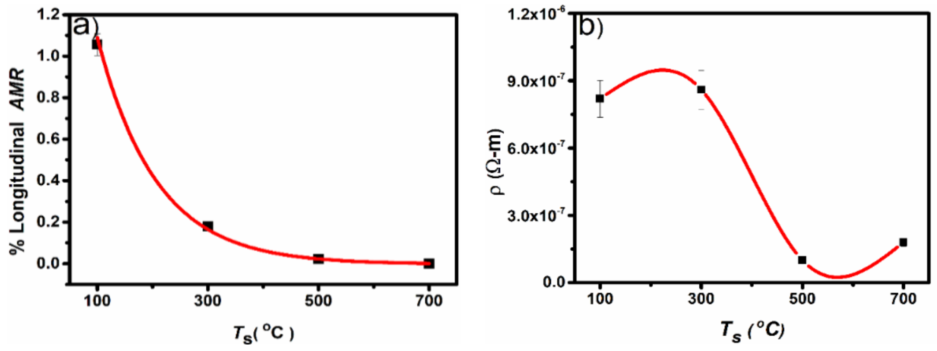

Fig. 4. The variation of (a) longitudinal % AMR and (b) ρ_{xx} of thin films vs T_s

4. Conclusions

Using pulsed laser deposition nickel thin were deposited on Si (100) substrate at four different temperatures 100 ºC, 300 ºC, 500 ºC and 700 ºC. Grain size, roughness and thickness were increased at higher deposition temperatures. Magnetic parameters like saturated magnetization (*Ms*), magnetic moment (*Mr*), coercivity (*Hc*) and residual magnetic ratio (*Ms/Mr*) strongly depends on the substrate temperate and were decreased with increased T_S from 100 ºC - 700 ºC. Electrical resistivity and anisotropic magneto resistance (AMR) of nickel thin films was measured with Vander Pauw four-point technique at room temperature. At high substrate-temperature, electrical resistivity was dropped from 0.82- 0.10 μ Ω-m. Both the transverse and longitudinal mode of magneto resistances of thin films were decreased at higher T_S.

Acknowledgments

This research work is partially supported by Higher Education Commission (HEC) of Pakistan under Project No: 20-1868/R & D/105754. M. Nawaz Rizwan acknowledges HEC Pakistan for financial support of six months visit to University of the Bristol, UK under international research support initiative programe (IRSIP).

References

[1] H. Gleiter, Acta Mater. **48**, 1 (2000).
[2] M. E. McHenry, D. E. Laughlin, Acta Mater. **48**, 223 (2000).
[3] H. Gleiter, Progress in Mater. Sci. **33**, 223 (1989).
[4] S. J. Henley, C. H. P. Poa, A. A. D. T. Adikaari, C. E. Giusca, J. D, Carey, S. R. P. Silva, Appl. Phys. Lett. **84**, 40 (2004).
[5] Anca Largeanu, G. O. Pompilian, D. G Galusca, Maricel Agop and Sliviu Gurlui. U.P.B. Sci. Bull. Series A **73**, 196 (2011).
[6] W. Kreuzpaintner, M. Störmer, D. Lott, D. Solina, A. Schreyer, Jounal of applied science **104**, 1 (2008).
[7] B Geetha Priyadarshini, S. Aich, M. Chakraborty, J. Mater. Sci. **46**, 2860 (2011).
[8] Y. Pauleau, S. Kukielka, W. Gulbinski, L. Ortega, S. N. Dub, J. Phys. D: Appl. Phys. **39**, 2803 (2006).
[9] N. Radic, P. Dubeik, S. Bemstorff, I. Djerdj, A. M. J. Appl. Cryst. **40**, 377 (2007).
[10] Thomas Otito, Georgees-Ivo Ekosse, Sathiaraj, T. Stephen, J. Appl. Sci. Eviron. Manage. **11**(2), 57 (2007).
[11] Prashant Kumar, Nanoscale Res. Lett. **5**, 1596 (2010).
[12] Mohammaed T. Hussein, Eman M. Nasir, Addnan H. Al-Aarajiy, Advance in material physics and chemistry **3**, 113 (2013).
[13] M. A. Vidales-Hutado, A. Mendoza-Galvan, Materials Chemistry and Physics **107**, 33 (2008).
[14] A. Hattar, D. M. Follstaedt, J. A. Knapp, I. M. Roberston, Acta Material **56**, 796 (2008).
[15] Amrut S. Lange, Satish J. Sharma, Ramchandra B. Pode, Archives of physics research **1**, 49 (2010).
[16] Hao-Long Chen,Yang-Ming Lu, Weng-Sing Hwang, Materials Transaction **46**, 872 (2005).
[17] Yuanqing He, Xuegeng Li, Mark T. Swaihart, Chem. Mater. **17**, 1017 (2005).
[18] C. J. Tsai, K. H. Yu, Thin Solid Films **350**, 91 (1999).
[19] Y. Suzuki, R. B. Van Dover, E. M. Gyorgy, Julia M. Philips, V. Korenivski, D. J. Werder, C. H. Chen, R. J. Cava, J. J. Krajewski, W. F. Peck, Jr. K. B. Do, Ginzton Laboratory, Standford University, Standford, California 94305-4085, (1995).
[20] Prashant Kumar, M Ghanashyam Krishna, A. K Bhattacharya. Bull Mater. Sci, **32**(3), 263 (2009).

[21] Pouyan Motamedi, Ken Bosnick, Kai Cui, Kenneth C. Cadien, James Hoyan, ACS Appl. Mater. Interfaces **9**(29), 24722 (2017).
[22] J. B. Yia, Y. Z. Zhoua, J. Dinga, G. M. Chowa, Z. L. Dongb, T. White, XingYu Gao, A.T.S. Wee, X. J. Yu, Journal of Magnetism and Magnetic Materials **284**, 303 (2004).